New Prognostic Method Based on Spectral Analysis Techniques Dealing with Motor Static Eccentricity for Aerospace Electromechanical Actuators

New Prognostic Method Based on Spectral Analysis Techniques Dealing with Motor Static Eccentricity for Aerospace Electromechanical Actuators

D: BELMONTE, M. D. L. DALLA VEDOVA, and P. MAGGIORE
Department of Mechanical and Aerospace Engineering
Politecnico di Torino
Corso Duca degli Abruzzi 24 – 10129, Turin
ITALY
matteo.dallavedova@polito.it

Abstract: - The prognostic algorithms are important to identify the precursors of incipient failures of electromechanical actuators (EMA) applied to aircraft primary flight controls. Keeping in mind the risk related to the performed functions of these actuators the anticipation of an incoming failure is really useful: a correct interpretation of the failure degradation pattern, in fact, can trig an early alert of the maintenance crew, who can properly schedule the servomechanism replacement, increasing the aircraft safety and reliability. In this paper the authors propose an innovative prognostic model-based approach, able to recognize the symptoms of an EMA degradation before the explicit exhibition of the anomalous behavior. The identification/evaluation of the considered incipient failures is performed analyzing proper critical system operational parameters, able to put in evidence the corresponding degradation path, by means of a numerical algorithm based on spectral analysis techniques. Subsequently, these operational parameters are correlated with the actual health condition of the considered system by means of failure maps created by a reference monitoring model-based algorithm. In the present work, the proposed method has been applied to an EMA with a brushless DC motor affected by a progressive increase of the static eccentricity of the rotor. In order to evaluate the performances of the aforesaid prognostic method a test simulation environment, able to manage different failure modes, has been defined. This numerical test case simulates the dynamic behaviors of the EMA taking into account nonlinear effects related to different kinds of progressive mechanical failures (such as transmission backlash, friction, and rotor static eccentricity). Results show that the method exhibit adequate robustness and a high degree of confidence in the ability to early identify a malfunctioning, minimizing the risk of fake alarms or unannounced failures.

Key-Words: - BLDC Rotor Static Eccentricity, Electromechanical Actuator (EMA), Prognostics and Health Management (PHM), Prognostic Precursors, Progressive Failures, Spectral Analysis

1 Introduction

Actuators provide a mechanical power transforming of electrical, pneumatic or hydraulic sources of power, and they are commonly used for driving flight control surfaces and utility aircraft subsystems. Flight control systems are critical for safety indeed they must meet severe reliability requirements of less than one catastrophic failure per 10^5 flight hours. The design of critical components such as actuators used for primary flight controls must respect the applicable Airworthiness Code (EASA CS-25, AMC 25.629) by a conservative safe-life approach which imposes proper levels of reliability and programmed removal of related components after a specific interval of time or operating cycles. Historical records indicate that the actual use is often very different from the estimated one, because the aforesaid design criterion is not able to evaluate possible initial flaws (e.g. occurred during manufacturing) and other impacting factors such as extreme or unanticipated operating scenarios, pilot and flying style in manned systems. Statistical based preventive maintenance tasks are also involved to remove components with significant useful life increasing costs and related inefficiencies. Prognostic is a discipline with the purpose to predict when a certain component loses its functionalities and is not further able to operate or to meet desired performances. It is based on analysis and knowledge of possible failure modes and on capability to identify incoming faults, due to aging or wear, by monitoring specific operational parameters (prognostic precursors) [1]. Prognostics is used in other technological fields and could be very useful to condition based maintenance, since it reduces both costs and inspection time.

To improve these advantages, a new discipline called Prognostics and Health Management (PHM) was born to provide real-time data on current health status of the system and to calculate Remaining Useful Life (RUL) before a fault or failure occurs, when a component becomes unable to perform its features at designed levels. The need for condition based maintenance is clearly recognized, but it is difficult to define robust PHM algorithms due to complex actuators phenomenology. It is necessary to develop a robust health management solution able to perform reliable and acceptable faults detection and failure prediction analyzing multiple, competitive failures modes by monitoring physically meaningful parameters [1].

Several aircraft use electrohydraulic (EHA) or simply hydraulic actuators for primary flight control system, but incoming Unmanned Autonomous Vehicles (UAVs) already utilize electromechanical actuators (EMA). Moreover, several research programs are introducing EMA in future military and civil flight control systems: as an example in 2011 the Sagem company has developed an EMA for the aileron on an Airbus A320 commercial jetliner. Typically PHM strategies are easier to implement on EMA since additional sensors are usually not required providing to define the health status of the system. The same sensors framework used for control schemes and systems monitor is also used in many PHM algorithms in a model based approach for health system evaluation.

This paper presents a study focused on the development a prognostic technique able to identify proper failure precursors alerting that degrading performances of an aeronautical electromechanical actuator exhibiting an anomalous behavior due to wear phenomena. In particular, three kinds of non-linear physical behaviors are considered: friction, backlash, rotor static eccentricity.

To assess the robustness of the proposed techniques, based on a typical Spectral Analysis approach, an appropriate simulation test environment has been developed. Simulations have then been run with progressive Static Rotor Eccentricity while the EMA model is subjected to different parameters configuration; the algorithms correctly sort out the failure precursors and make a correlation between the actual Static Eccentricity percentage and the calculated operating maps to identify and evaluate incoming failure.

Results show that an adequate robustness and confidence has been gained in the ability to early identify the EMA malfunctioning minimizing the risk of false alarms or unannounced failures.

The aims of this work are:

1. The proposal of a numerical algorithm, implemented in MATLAB-Simulink simulation environment, able to perform the simulations of dynamical systems for EMA taking into account evaluation of rotor static eccentricity due to progressive bearings wear.
2. The proposal an innovative prognostic method introducing typical spectral signal analysis techniques able to detect, by specific failure precursors, an accurate health state of the flight control systems.

2 Primary Flight Control EMAs

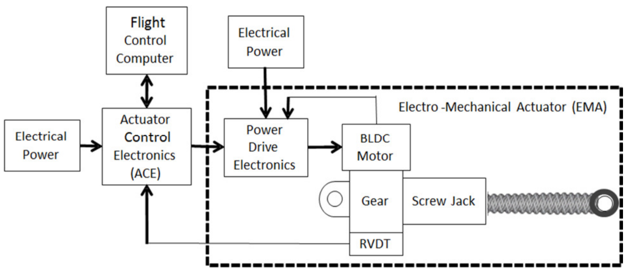

Fig. 1: Electromechanical actuator (EMA) scheme.

Primary flight controls are typically proportional servomechanisms with continuous activation: they must return a force feedback related to command intensity and a high frequency response. Since their loss is a critical issue, their reliability must be very high. Their purpose is to control the dynamic of the aircraft by generating, by means of the rotation of the related aerodynamic surfaces, unbalanced forces/couples acting on the aircraft itself. These controls are usually conceived to obtain the aircraft rotation around one of the three body axis when one control surface is activated. This kind of actuator, because of its great accuracy, high specific power and very high reliability, is often equipped on current aircrafts, even if on more modern airliners electro-hydrostatic actuators (EHA) or electro-mechanical actuators (EMA) are installed. In the last years the trend towards the all-electric aircrafts brought to an extensive application of novel optimized electrical actuators, such as the electromechanical ones (EMA). To justify the fervent scientific activity in this field and the great interest shown by the aeronautical world, it must be noticed that, compared to the electrohydraulic actuations, the EMAs offer many advantages: overall weight is reduced, maintenance is simplified and hydraulic fluids, which is often contaminant, flammable or polluting, can be elimination.

For these reasons, as reported in [2], the use of actuation systems based on EMAs is increasing in various fields of aerospace technology. As shown in Fig. 1, a typical electromechanical actuator used in a primary flight control is composed by:

1. An actuator control electronics (ACE) that closes the feedback loop, by comparing the commanded position (FBW) with the actual one, elaborates the corrective actions and generates the reference current I_{ref};
2. A Power Drive Electronics (PDE) that regulates the three-phase electrical power;
3. An electrical motor, often BLDC type.
4. A gear reducer having the function to decrease the motor angular speed and increase its torque.
5. A system that transforms rotary motion into linear motion: ball screws or roller screws are usually preferred to acme screws because, having a higher efficiency, they can perform the conversion with lower friction;
6. A network of sensors used to close the feedback rings (current, angular speed and position) that control the whole actuation system (reported in Fig. 1, as RVDT).

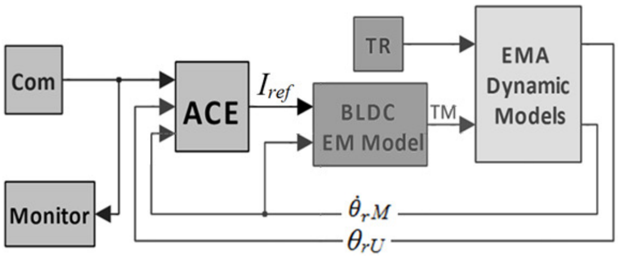

Fig. 2: Proposed EMA block diagram.

3 Proposed EMA Numerical Model

As previously mentioned, goal of this research is the proposal of a new a technique to identify precocious symptoms (usually defined failure precursors) of EMA degradations. In order to assess feasibility performance and robustness of the aforesaid technique, a suitable simulation test environment has been developed in the MATLAB/Simulink.

The proposed numerical model (Fig. 2), widely described in [3], is consistent with the considered EMA architecture. As shown in Fig. 2, the propose simulation model is composed by six subsystems:

1. *Com*: input block that generates the different position commands.
2. *ACE*: subsystem simulating the actuator control electronics, closing the feedback loops and generating in output the reference current I_{ref}.
3. *BLDC EM Model*: subsystem simulating the power drive electronics and the trapezoidal BLDC electromagnetic model, that evaluates the torque developed by the electrical motor as a function of the voltages generated by three-phase electrical regulator.
4. *EMA Dynamic Model*: subsystem simulating the EMA mechanical behavior by means of a 2 degree-of-freedom (d.o.f.) dynamic system.
5. *TR*: input block simulating the aerodynamic torques acting on the moving surface controlled by the actuator .
6. *Monitor*: simulates the monitoring system.

It must be noted that this numerical model is able simulate the dynamic behavior of the considered EMA taking also into account the effects of BLDC motor non-linearities [4-8], mechanical end-of-travels, compliance and backlashes acting on the mechanical transmission [9], analogic to digital conversion of the feedback signals, electrical noise acting on the signal lines and electrical offset of the position transducers [10] and dry friction (on bearings, gears, hinges and screw actuators) [11].

4 EMA Failures and Performance Degradations

Only recently EMAs have been employed in aeronautics for flight control systems, so the cumulate flight hours and the on-board installation periods don't permit reliable statistic data about recurring failures. Generally it is possible to classify among four main failures categories: mechanical or structural failures, BLDC motor failures, electronics failures and sensor failures. The present work takes into account effects of mechanical failures due to progressive wear focused on progressive static rotor eccentricity related to bearing wear.

Electrical and sensor failures have not a secondary importance, but their evolution is very fast, nearly instantaneous, so corresponding failure precursors are often hard to identify and evaluate; nevertheless it is intention of the authors to study these kind of failures in a next work.

As is known, wear increases the dry friction phenomena that occur between two surfaces in relative motion, increasing both static and dynamic friction coefficients. The driven system requires higher torques to actuate the control surface with the same external load. Even if an increased dry friction does not cause seizure of the entire system, it reduces the corresponding servomechanism accuracy and sometimes it generates dynamic unexpected responses, as stick-slip or limit cycles due to the interaction between PID controller and friction forces. The mechanical wear could also generate backlash in EMA moving parts such as gears, hinges, bearings and especially ball screw actuators; these backlashes, acting on the elements of the mechanical transmission, reduce the EMA accuracy and, as a function the mutual position with respect to the signal transducers, can lead to problems of dynamic stability and controllability of the whole actuator. The eccentricity fault of a stator and rotor is due mainly to mechanical reasons. In this kind of failures, the axes of symmetry of the stator and of the rotor and the rotational axis of rotor are displaced to each other. This displacement of symmetrical axes can be classified into static, dynamic and mixed eccentricities [12]; in this work, only the first type of eccentricity will be discussed.

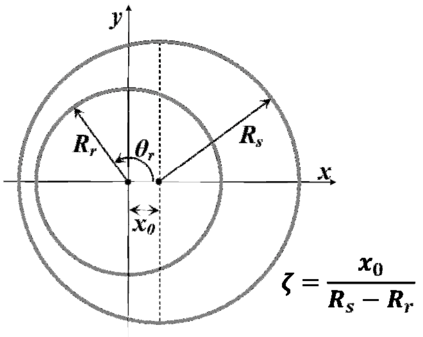

Fig. 3: Reference system for the definition of rotor static eccentricity ζ.

The static eccentricity (Fig. 3) consists in a misalignment between the rotor rotation axis and the stator axis of symmetry; the rotor is symmetric and rotates towards its rotation axis, this misalignment initially is mainly due to manufacturing tolerances and imperfections, but, during operational period, increases as a consequence of wear in bearings that support rotor shaft. When this failure occurs in multipolar motor, the rotor generates a magnetic flux that has not cyclic symmetry, since the air gap varies during its 360° degrees turn. Therefore, if a rotor has an evaluable static eccentricity, an additional radial force component arises and its magnitude varies like a sine wave. In condition of Static Eccentricity the air gap is not constant and symmetric along rotor turn (Fig. 3), so the clearance between the rotor and the stator can be mathematically represented by this function:

$$g'(\vartheta) = g_0 + x_0 \, cos(\vartheta) \qquad (1)$$

where g_0 is the initial clearance without misalignment and the second term added represents the sinusoidal air gap variation as a function of the misalignment x_0. In terms of motor performances, in these conditions the provided torque is lower than in nominal conditions (because of a change in the electromagnetic characteristics of the engine): to simulate eccentricity effects avoiding more complex electromagnetic FEM models, a smart numerical algorithm has been released. Since static eccentricity modifies the magnetic coupling between the stator and the rotor, the proposed algorithm adjusts the angular modulation of the back-EMF coefficients and thereby the related torque constants. As reported in [2], this algorithm is implemented by means of the functions *f (u)* contained in the BLDC EM Model block of Fig. 2 and acts on the three back-EMF constants *Cei* (one for each of the three phases) modulating their trapezoidal reference values *Kei* as a function of coil short circuit percentage, static rotor eccentricity ζ and angular position ϑr.

$$\text{e\_a} = \text{Ke}_\text{i} \cdot \text{Ce}_\text{i} \cdot (1 + \zeta \cdot \cos(\vartheta_\text{r})) \qquad (2)$$

The obtained constants (*ke_a*, *ke_b*, *ke_c*) are then used to calculate the corresponding counter-electromotive forces (*ea*, *eb*, *ec*) to evaluate the mechanical couples (*Cea*, *Ceb*, *Cec*) generated by the three motor phases. The effects of the aforesaid failures will be briefly analyzed in the next section, in which the related EMA simulations will be examined. With respect to other EM models available in literature, the numerical model shown in the previous sections is able to calculate the instantaneous value of each current phase (*Ia*, *Ib*, *Ic*) also in case of unbalanced electromagnetic system (e.g. partial short circuit on a stator branch or rotor static eccentricity). Then, it is possible correlate the progressive static eccentricity with these currents (used as failure precursors) by means of an algorithm, based on the Fourier spectral analysis, that analyses the filtered phase currents; for this purpose, each phase current is filtered by three low pass signal filter, in order to attenuate noise and disturbances [13]. The Fourier Transform (FT) is a mathematical instrument that changes the time domain representation into a frequency domain representation, which has many applications in physics and engineering. The FT comes from a study of Fourier series that it represents complicated but periodic functions as infinite sum of sine and cosine functions with different amplitude and phase.

It's possible to represent sine and cosine formulas using Euler's Formulas, then the Fourier Series is written by (3):

$$f(x) = \sum_{n=-\infty}^{+\infty} c_n e^{2\pi i\left(\frac{n}{T}\right)x} \quad (3)$$

where c_n is the n-th Fourier coefficient.

The Discrete Fourier Transform (DFT) is the equivalent of Continuous Fourier Transform for a signal known only at N samples time during a finite Time acquisition [14], so we have a finite sequence data considering the signal periodic as:

$$F[n] = \sum_{k=0}^{N-1} f[k] e^{-j\frac{2\pi}{N}nk} \quad (4)$$

The DFT approximates the Fourier Transform since it provides only for a finite set of frequencies during a limited acquisition time. It must be noted that there are two main types of DFT calculation errors: "Aliasing"[1] and "Leakage". According to the Nyquist-Shannon theorem, defined f_M the upper limit of the frequency bandwidth of a signal, in order to avoid "Aliasing" phenomena during DFT calculation, the Sampling Frequency f_S must be defined as:

$$f_s > 2f_M \quad (5)$$

In the present work, in order to avoid Aliasing errors, the performed DFT uses a sampling frequency f_S equal to the inverse of the integration time DT of EMA simulation model: this requisite allows the representation of all high frequency components calculated by the model EMA.

The continuous Fourier Transform of a waveform requires the integration to be performed over the interval -∞ to +∞ or over an integer number of cycles of the waveform. If we attempt to calculate the DFT over a non-periodic signal, we have a corrupted frequency transform due to "Leakage" errors. For most waveform of real data it is not possible to reduce "Leakage" without a specific data modification.

This used solution is usually called "Windowing" [16]: a cosine function is applied over the entire signal to taper the samples towards zero at both endpoints without discontinuity with a hypothetical next period.

1 It must be noted that we have "Aliasing" DFT calculation errors when the samples are not sufficiently closely spaced to represent high frequency spectral components.

Rather than performing a DFT calculation, a FFT calculation is often preferred to reduce the number of involved multiplications [17-19]. The proposed numerical module uses a FFT with a "Hanning" windows: this type of windowing, often used for general purpose applications in spectral analysis [15], is defined as:

$$Wn = \frac{1}{2}\left\{1 - cos\left[\frac{2\pi n}{(N-1)}\right]\right\}; \quad (6)$$

where $0 \leq n \leq (N-1)$.

Windowing have a side effects because data are reduced and set to zero at the beginning and end of each time record to force the signal to be periodic; it must be noted that there is no loss in amplitude readout accuracy, but a loss in frequency resolution is present. A processing technique called "overlap" is able to enhance events occurring near the beginning and ending of time record. The entire simulation time is divided in several time section intervals, which are not time sequential but overlapped of 67% from the first time section in order to improve spectral information. Energy information in signal must be preserved during transformation. That is, the energy measured on time signal must equal the energy measured on the frequency representation of that signal.

All the aforesaid spectral techniques (and the related requisites) are merged together and implemented into the proposed numerical module called EMA Spectral Algorithm. This module processes all filtered phase currents deriving from each considered value of the rotor static eccentricity and correlates these failures with the corresponding failure precursors, generating a simulated "operating map". Once defined, for each type of EMA examined, its own "operating maps" it is possible to conceive dedicated fault detection/evaluation systems (on-board systems or portable devices equipped with embedded versions of the proposed spectral analysis algorithms) able to evaluate static rotor eccentricity during preflight test.

5 EMA Spectral Algorithm and Operating Maps

Simulation EMA environment works with step command with a very high position value for driving surface to quickly saturate the electromechanical actuator, that after a short transient time, it reaches the max velocity without aerodynamic load.

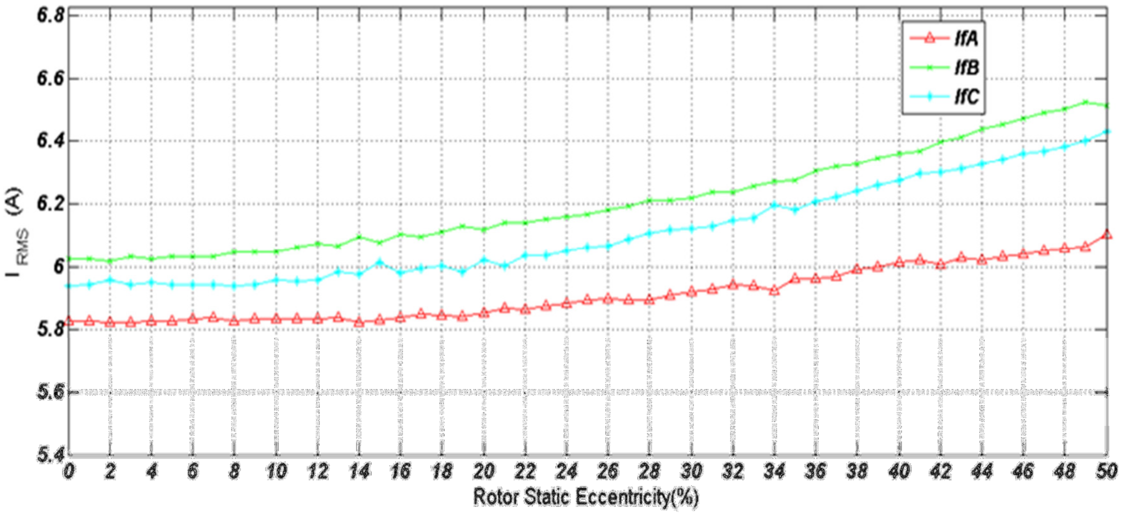

Fig. 4: Evolution of RMS currents as a function of rotor static eccentricity ζ.

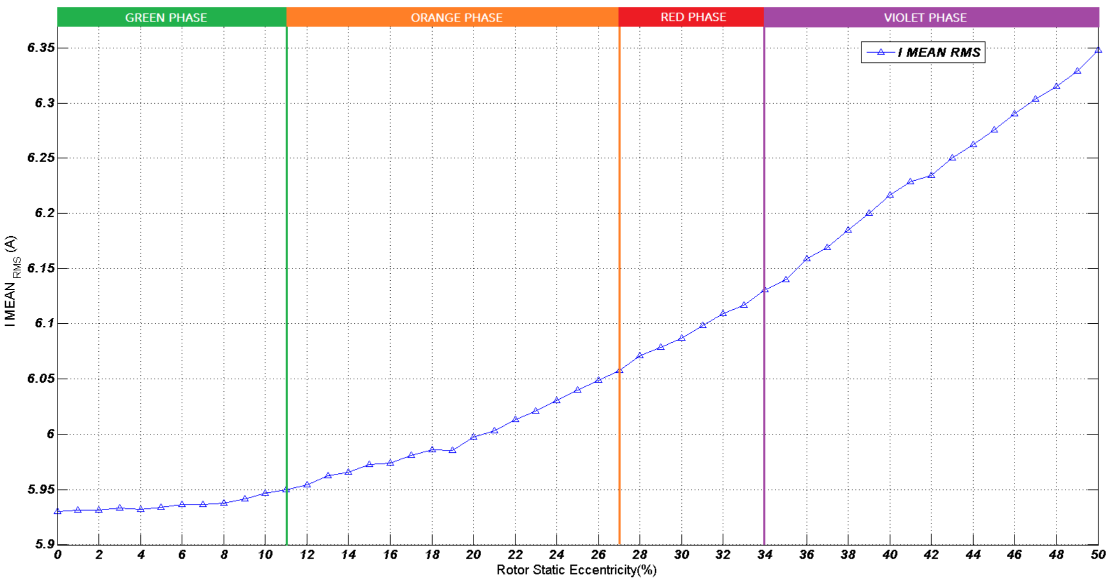

Fig. 5: Evolution of mean value of RMS currents as a function of rotor static eccentricity ζ.

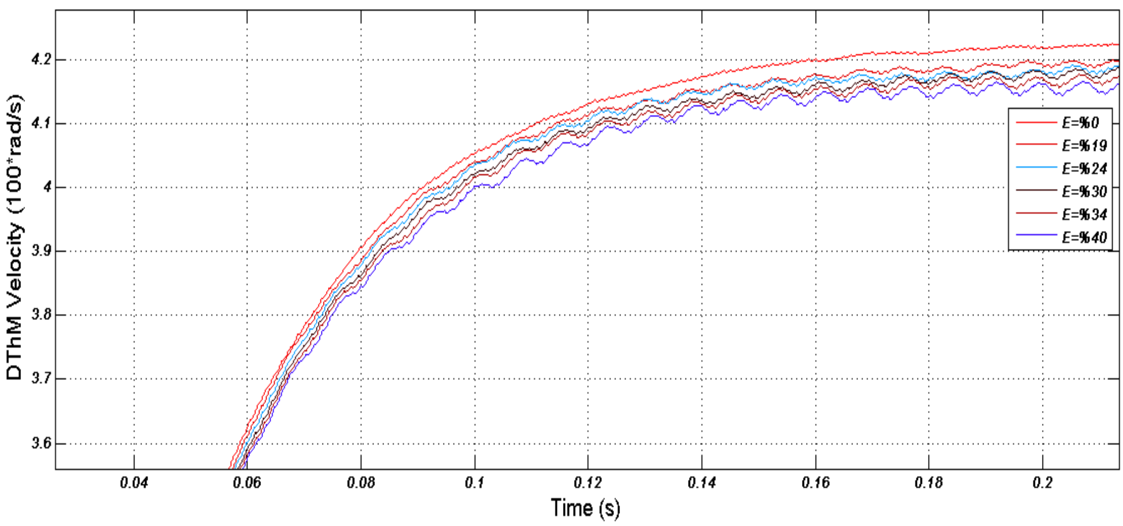

Fig. 6: Zoom on Actuator Velocity as function of Simulation Time and rotor static eccentricity ζ.

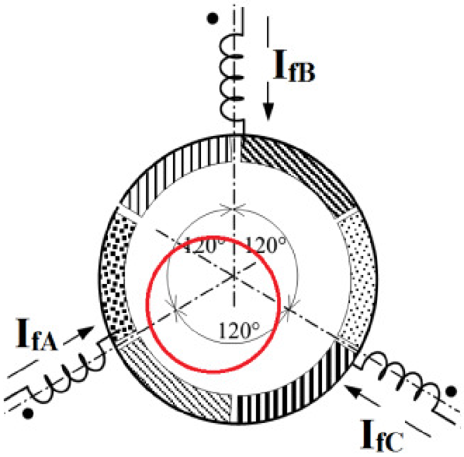

Fig. 7: Rotor Static eccentricity ζ (indicated by Red Rotor Position) and filtered phase currents in generic three phase configuration

The entire simulation time test amounts to one second and, for each simulated actuation test, all filtered phase currents (I_{fA}, I_{fB}, I_{fC}) are acquired. These filtered current signals, expressed as a function of simulated time, are divided in intervals called "time sections" of 25% of the simulation time and, sequentially, a FFT single sided spectral analysis (according to the Cooley Tukey algorithm [17]) is performed for each time section. To improve the frequency resolution of the algorithm, the time sections are extracted using overlap processing so, during one second of acquired signal, more time sections are post-processed [20]. Thus, a set of FFT spectral diagrams is calculated; the meaningful harmonics are identified by means of a peak hold function that, for each frequency line, finds the maximum magnitude peaks between all spectral diagrams that are extracted for each filtered phase current. The comparison among the sets of max magnitude peaks found in each filtered phase current reveals that from 0% to 33% of static rotor eccentricity the first max magnitude peak has the same constant frequency value called Hz1 (Hz1= 33.568 Hz). After this percentage of static rotor eccentricity, the first magnitude peak for each filtered phase current switches to another constant frequency value called Hz2 (Hz2= 32.805 Hz); this means that, when the static eccentricity is equal to a given percentage of the clearance between rotor and stator, the frequency of the first maximum magnitude peak decreases (Hz1>Hz2). The Root Mean Square (RMS, also known as the quadratic mean) of a given signal time history is a measure of overall energy and it is often used to extract signal features for prognosis and trending data.

In order to avoid numerical problems, the time history of the considered signal must be digitized at a particular sample rate (for N samples), then RMS value can be estimated by:

$$rms = \sqrt{\frac{1}{N}\sum_{i=1}^{N} x(i)^2} \tag{7}$$

For each filtered phase current (I_{fA}, I_{fB}, I_{fC}) a RMS value is calculated processing the rotor static eccentricity values from 0% to 50% with 1% increasing step; the results are three signals, called I_{A_RMS}, I_{b_RMS} and I_{c_RMS}, evolving as shown in Fig. 4. The progressive eccentricity causes progressive asymmetry of the magnetic field so the RMS filtered phase current values increase and, therefore, the torque needed to maintain the same actuator velocity increase. The progressive eccentricity causes progressive asymmetry of the magnetic field so the RMS filtered phase current values increase, as shown in Fig. 4 and, similarly, the actuation velocity decrease as shown in Fig. 6. In brushless motor actuator velocity is related to voltage supply of the stator phases then the same actuator velocity is related to the same voltage supply on the three rotor phase as showed in Fig. 7. The filtered phase currents are similarly related to torque applied on rotor component considering external load and friction forces. Electrical power, supplied by brushless motor, is generally indicated as multiplication between current and voltage, under the same nonlinear friction and external loads. Analyzing RMS values of the EMA simulation model, as failure precursors, it is possible to define some important features about involving of filtered phase currents with clearance distribution between rotor and stator component as showed in Fig. 3. The phase current I_{fA} is particular because to maintain the same actuator velocity, it requires less RMS current value for each progressive static eccentricity value than the other phase I_{fB} and I_{fC} as showed in Fig 4. Indeed I_{fA} is involved in minimum clearance, between stator and rotor component, so minimum magnetic resistor is related to minimum required power to the phase current considering the same actuator velocity for all the current phases (I_{fA}, I_{fB}, I_{fC}). With the same above considerations the filtered phase current I_{fB} is involved in maximum clearance between stator and rotor component, so globally maximum magnetic resistor is related to maximum required power to the phase current considering the same actuator velocity.

As shown in Fig. 5, evaluating the mean value of the RMS of filtered phase currents, calculated for each of the considered eccentricity percentage ζ, it is possible to perform an evaluation of the EMA health conditions, defining several operating intervals related to specific eccentricity percentages:

Green Phase: from 0% to 10% of the rotor static eccentricity (with respect to the stator-rotor air gap); this operating interval corresponds to Normal Mode with acceptable actuator performances; it is related to a negligible static eccentricity, mainly due to tolerances of manufacturing and beginnings of mechanical wear. It must be noted that, with respect to reference value mean RMS on 0% static eccentricity, it has a wide interval about 16 mA;

Orange Phase: from 11% to 26% of the rotor static eccentricity percentage; this operating interval corresponds to Moderate Mode with actuator performances related to incoming evaluable command degradations. Respect to reference value mean RMS on 11% static eccentricity this phase has a wide interval about 100 mA;

Red Phase: from 27% to 33% of the rotor static eccentricity; this operating interval corresponds to Serious Mode where actuator performances are degraded and condition based maintenance operations need to be planned. With respect to reference value mean RMS on 27% static eccentricity, it has a wide interval about 60 mA;

Violet Phase: from 34% to 50% of the rotor static eccentricity; this operating interval corresponds to Extreme Mode. In this case the actuator performances are much degraded and the based maintenance operations are needed as soon as possible. With respect to reference value mean RMS on 34% static eccentricity, this violet phase has a wide interval about 200 mA.

6 Conclusions

The proposed model-based approach allows the calculation of specific operating maps for many different EMA models: in fact, modifying defined sets of technical parameters, it is possible to adapt the performances of the numerical system to a given type of EMA and therefore to define the corresponding operational map. Actual EMA failure precursors, directly acquired by on-board maintenance systems, are compared with the corresponding calculated operating map in order to evaluate, during a preflight test, the percentage of static rotor eccentricity avoiding degraded flight command performances.

Once defined the operational maps simulating EMA model, integrated with the authors spectral numerical module, it is possible to have an adequate accuracy to individuate the health state of the actual actuator by performing pre-test flight as indicated in previous paragraphs. Results are encouraging the extension of the proposed technique to investigate more challenging occurrences, such as the electrical and sensor failures, for which the evolutions are usually very fast, if not instantaneous, and the corresponding failure precursors are often difficult to identify and evaluate. For this purpose the actuator model should be further detailed and new element should be modelled. Combined failures should also be investigated.

References:

[1] M. D. L. Dalla Vedova, P. Maggiore, L. Pace. Proposal of Prognostic Parametric Method Applied to an Electrohydraulic Servomechanism Affected by Multiple Failures. *WSEAS Transactions on Environment and Development*, ISSN: 1790-5079, pp. 478-490.

[2] M. Battipede, M.D.L. Dalla Vedova, P. Maggiore, S. Romeo, Model based analysis of precursors of electromechanical servomechanisms failures using an artificial neural network, *AIAA Modeling and Simulation Technologies Conference,* Kissimmee, Florida, 2015.

[3] P. Maggiore, M.D.L. Dalla Vedova, L. Pace, A. Desando, Definition of parametric methods for fault analysis applied to an electromechanical servomechanism affected by multiple failures, *Second European Conference of the PHM Society 2014 (PHME'14)*, Nantes, France, 8-10 July 2014, pp. 561-571.

[4] M. Çunkas, O. Aydoğdu, Realization of Fuzzy Logic Controlled Brushless DC Motor Drives using Matlab/Simulink, *Mathematical and Computational Applications*, 2010, Vol.15, pp. 218-229.

[5] A. Halvaei Niasar, H. Moghbelli, A. Vahedi, Modelling, Simulation and Implementation of Four-Switch Brushless DC Motor Drive Based On Switching Functions, *IEEE EUROCON 2009*, St.-Petersburg, Russia, 2009, pp. 682-687.

[6] B.K. Lee, M. Ehsani, Advanced Simulation Model for Brushless DC Motor Drives, *Electric Power Components and Systems*, Vol.31, No.9, 2003, pp. 841–868, ISSN: 1532-5008.

[7] T. Hemanand, T. Rajesh, Speed Control of Brushless DC Motor Drive Employing Hard Chopping PWM Technique Using DSP, *Proceedings of India International Conference on Power Electronics (IICPE 2006),* 2006.

[8] T.A. Haskew, D.E. Schinstock, E.M. Waldrep, Two-Phase On' Drive Operation in a Permanent Magnet Synchronous Machine Electromechanical Actuator, *IEEE Transactions on on Energy Conversion,* Vol.14, No.2, 1999.

[9] L. Borello; G. Villero, M.D.L. Dalla Vedova. New asymmetry monitoring techniques: effects on attitude control, *Aerospace Science and Technology*, Vol.13, No.8, 2009, pp. 475-487.

[10] L. Borello, M.D.L. Dalla Vedova, G. Jacazio, M. Sorli, A Prognostic Model for Electrohydraulic Servovalves, *Annual Conference of the Prognostics and Health Management Society*, San Diego, CA, 2009.

[11] L. Borello, M.D.L. Dalla Vedova, A dry friction model and robust computational algorithm for reversible or irreversible motion transmission, *International Journal of Mechanics and Control*, Vol.13, No.2, 2012, pp. 37-48.

[12] M. Akar, S. Taskin, S. Seker, I. Cankaya, Detection of static eccentricity for permanent magnet synchronous motors using the coherence analysis, *Turkish Journal of Electrical Engineering & Computer Science*, Vol.18, No.6, 2010, pp. 963-974.

[13] E. E Ngu, K. Ramar, R. Montano, V. Cooray, Fault characterisation and classification using wavelet and fast Fourier transforms, *WSEAS Transactions on Signal Processing*, Vol.4 No.7, July 2008, pp. 398-408.

[14] A. V. Oppenheim, R. W. Schafer, J. A. Buck, *Discrete-time signal processing*. Upper Saddle River, N.J.: Prentice Hall. 1999, pp. 468–471.

[15] F. Harris, On the use of Windows for Harmonic Analysis with the Discrete Fourier Transform. *Proceedings of the IEEE*, Vol.66, No.1, 1978, pp. 51-83.

[16] W. Hongwei, Evaluation of Various Window Functions using Multi-Instrument, *Virtins technology*, May 2009. http://www.virtins.com/

[17] J.W. Cooley, J.W. Tukey, An algorithm for the machine calculation of complex Fourier series, *Mathematics of Computation*, Vol.19, No.90, 1965, pp. 297-301.

[18] D. F. Elliott, K. R. Rao, *Fast transforms: Algorithms, analyses, applications*, New York: Academic Press, 1982.

[19] W. Huaqing, C. Peng, Fault Diagnosis Method Based on Kurtosis Wave and Information Divergence for Rolling Element Bearings, *WSEAS Transactions on Systems*, Vol.8, No.10, October 2009, pp. 1155-1165.

[20] F. Ramian, *Implementation of Real-Time Spectrum Analysis*, Rohde & Schwarz, January, 2011.